Published by :
http://www.ijert.org

International Journal of Engineering Research & Technology (IJERT)
ISSN: 2278-0181
Vol. 9 Issue 06, June-2020

Numerical Studies on Short Concrete-Filled Double Skin Composite Tube Columns under Axially Compressive Loads by using ABAQUS/CAE 6.14

Saurabh Verma[1], Mr. Anish Krishnan[2], Mr. Shashikant Shrivastava[3], Dr. Satish Parihar[4]
[1]M. Tech Student, Department of Civil Engineering, FET, Rama University
[2]Assistant Professor, Prabhat Engineering College, Kanpur
[3]Assistant Professor,
[4]Head of Department,
Department of Civil Engineering, Faculty of Engineering & Technology,
Rama University, Kanpur, Uttar Pradesh 209217

***Abstract* – Concrete-filled double skin composite tube columns are special columns in which concrete is sandwiched between two tube structures. The outer tube is made of steel and the inner tube is PVC. Concrete-filled steel tubular (CFST) structure offers numerous structural benefits, and has been widely used in civil engineering structures. A numerical study of the behaviour of CFDSCT members under axially compressive loads using ABAQUS, where nonlinear material behaviour and strain rates of steel and concrete are included. The finite element analysis (FEA) models of CFDSCT members are described and verified using existing experimental results. A parametric study investigating the influence of different radius-to- thickness ratio, hollow section ratio, thickness of PVC-U pipe of the column under axially compressive load. The result shows that there is a good agreement between the experimental data and the finite element analysis data.**

I. INTRODUCTION

1.1 General- Concrete-filled steel tubes are important structural members in composite construction. The concrete-filled steel tubular (CFST) structure offers numerous structural benefits, including high strength and fire resistances, favourable ductility and large energy absorption capacity. There is also no need for the use of shuttering during concrete construction; hence, the construction cost and time are reduced. These members are economical and quicker to construct, compared to conventional concrete-reinforced columns. In multi-storey buildings, architects may detail downpipes or other services such as electrical wiring in the centre of the columns. This is done for aesthetic reasons. One way to achieving this is to use concrete-filled double skin tubes (CFDSTs). CFDSTs are structural members that have a double steel skin with concrete sandwiched between two steel tubes. These structural elements can be concrete-filled double skin rectangular tubes, concrete-filled double skin circular tubes, or concrete-filled double- skin rectangular-circular tubes. Similarly to CFTs, these members are economical and quicker to construct than conventional concrete-reinforced columns because the steel tube serves as form-work. This means that high rise buildings can be completed swiftly when CFDST columns are used. The concrete fill prevents the outer steel tube from buckling inwards whilst the steel prevents the concrete from deforming laterally, under compressive loads. CFDST columns have structural benefits similar to concrete-filled tube (CFT) columns. In addition they are lighter, stronger and possess better energy absorption.

1.2 Concrete-Filled double skin composite tube columns :- In the concrete-filled double skin tubes the main constraint on sandwiched concrete is from the outer skin tube. The function of the inner skin tube is mainly to provide a formwork although it can also help the outer skin tube and sandwiched concrete to sustain external compressive loads. From an economical point of view, the inner steel tube could be thinner than the outer skin steel tube. However, the thinner the steel tube the easier the steel tube can buckle. As an alternative, one may use other materials as the inner tube such as plastic tube if they can also provide a formwork for concrete construction. Here new type of concrete-filled double skin composite tubular column (CFDSCT) is proposed, in which the outer tube is steel and the inner tube is PVC-U pipe, which is different from the FRP steel-concrete hybrid columns.

1.3 Components of the g CFDSCT :- Three typical column cross-sections, where the concrete is filled in a circular hollow section (CHS), a square hollow section (SHS) or a rectangular hollow section (RHS), where D and B are the outer dimensions of the steel tube and t is the wall thickness of the tube. It is noted that the circular cross section provides the strongest confinement to the core concrete, and the local buckling is more likely to occur in square or rectangular cross-sections. However, the concrete-filled steel tubes with SHS and RHS are still increasingly used in construction, for the reasons of being easier in beam-to-column connection design, high cross-sectional bending stiffness and for aesthetic reasons. Other cross-sectional shapes have also been used for aesthetical purposes, such as polygon, round-ended rectangular and elliptical shapes, as shown in fig,

International Journal of Engineering Research & Technology (IJERT)
ISSN: 2278-0181
Vol. 9 Issue 06, June-2020

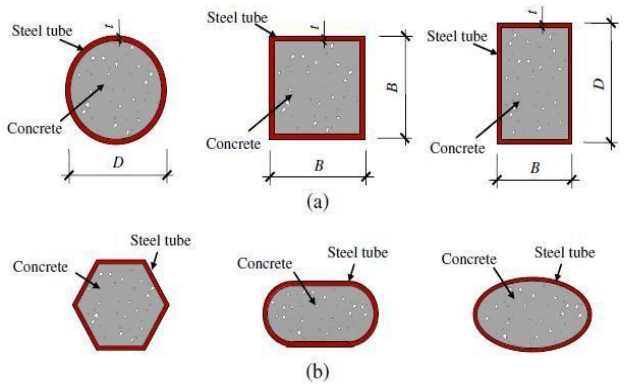

Fig 1.1: Typical concrete-filled steel tubular cross sections

It is well known that the compressive strength of concrete is much higher than its tensile strength. Furthermore, the compressive strength is enhanced under bi-axial or tri-axial restraint. For the structural steel, the tensile strength is high while the shape may buckle locally under compression. In concrete-filled steel tubular members, steel and concrete are used in such a way that their natural and most prominent characteristics are taken advantage of. The confinement of concrete is provided by the steel tube, and the local buckling of the steel tube is improved due to the support of the concrete core. Fig shows schematic failure modes for the stub column concrete-filled steel tubular column and the corresponding steel tube and concrete. It can be seen that both inward and outward buckling is found in the steel tube, and shear failure is exhibited for the plain concrete stub column. For the CFST, only outward buckling is found in the tube, and the inner concrete fails in a more ductile fashion.

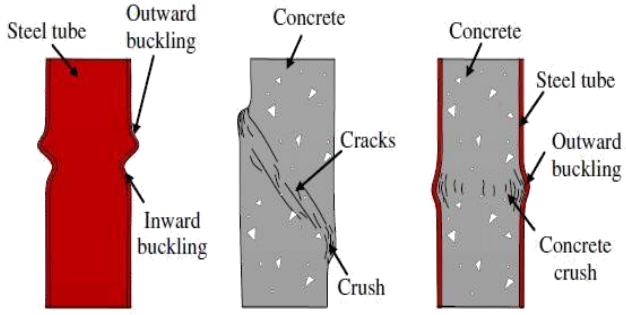

Fig 1.2: Schematic failure modes of hollow steel tube, concrete and CFST stub columns

Fig. shows a comparison of the measured results between a steel stub column, a reinforced concrete stub column and a concrete-filled steel tubular stub column without steel reinforcement, where D and t are the outer diameter and the wall thickness of the circular steel tube, respectively; fy is the yield strength of the steel; fcu is the compressive strength of the concrete cube.The term "steel tube + RC" in Fig. 3 indicates the summation of the ultimate strength of the steel tube and the reinforced concrete (RC) specimens. It clearly shows that the ultimate strength for a concrete-filled steel tube is even larger than the summation of the strength of the steel tube and the RC column, which is described as "1(steel tube) + 1 (concrete core) greater than 2 (simple summation of the two materials)". Fig. 3(b) shows a schematic view of the load versus deformation relationship of the hollow steel tube, the concrete stub column by itself and the concrete-filled steel tube. It can be seen that the ductility of the concrete-filled steel tube is significantly enhanced, when compared to those of the steel tube and the concrete alone.

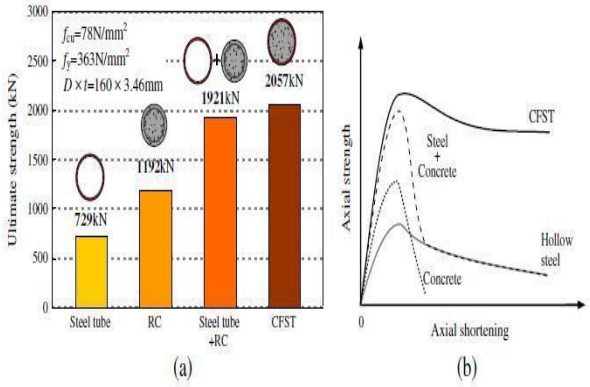

Fig 1.3: Axial compressive behaviour of CFST stub column

1.4 Types of Concrete-Filled steel structures :- Apart from the common concrete-filled steel tubes shown in Fig, there are other types of "general" member designations in the CFST family. Some of these are shown in Fig.4 i.e. concrete-filled double skin steel tubes (CFDST), concrete-encased concrete-filled steel tubes as well as reinforced and stiffened concrete-filled steel tubes.

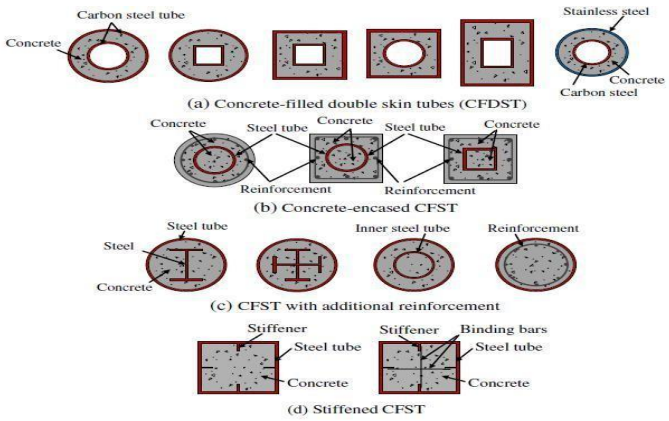

Fig 1.4: General CFST cross sections

The characteristics of these "general" CFST members are as follows (i) they consist of the steel tube(s) and the filled concrete (ii) the concrete and the steel tube(s) both sustain the axial load together.

International Journal of Engineering Research & Technology (IJERT)
ISSN: 2278-0181
Vol. 9 Issue 06, June-2020

1.5 Objective of study

An experimental study on the behaviour of concrete-filled double skin composite column under axially compressive load was carried out by W. Yuan and J. Yang [1]. Using the data from the experimental study, a model analysis has been carried out by using ABACUS.

The materials which were used in the experiments were concrete, steel and PVC-U pipe.

Concrete: The concrete used in the tested CFDSCT columns was mixed with a ratio of cement, sand, aggregate, and water as 0.91,1, 2.47 and 0.32. During mixing small amount of naphthalene super plasticizer was added to improve cement hydration process, the weight ratio of added plasticizer to the cement was about 1%. The concrete was filled in layers and was vibrated by a poker vibrator. The specimens were placed upright to air-dry until testing. During curing, a very small amount of longitudinal shrinkage occurred at the top of the columns. To ensure an even top surface high strength epoxy material was used to fill any possible longitudinal gap. While casting the specimens, three cubes of 150×150×150 mm were also casted and cured in the similar conditions as the tested specimens. The compressive strengths of the three cubes were obtained at 28 days, the average of which was 62.3 MPa. The modulus of elasticity of concrete was found to be 36.3 GPa, and Poisson's ratio is assumed to be 0.2.

Steel: It should be noted that various national standards contain structural steel designations, where the chemical composition and the mechanical properties may be different. However, these steel specifications are comparable in general. Various kinds of steel can be used in concrete- filled steel tubular members, such as normal carbon ("mild") steel, high strength steel, high-performance fire-resistant steel, weathering steel, etc. For the steel tubes, their properties must adhere to the steel material standards. The Young's modulus of 210 GPa, Yield stress of steel is 235 MPa, Ultimate strength of the steel is 375 MPa and poisson's ratio of steel is 0.3

PVC-U pipe: Polyvinyl chloride is a thermoplastics material which consists of PVC resin compounded with varying proportions of stabilisers, lubricants, fillers, pigments, plasticisers and processing aids. The PVC compounds with the greatest short-term and long-term strengths are those that contain no plasticisers and the minimum of compounding ingredients. This type of PVC is known as UPVC or PVC-U. PVC pipes retains its toughness even at lower temperatures. In addition PVC-U pipe exhibits very high fatigue resistance. Potential damage by repetitive variations in operating pressure (surges) is highly resisted. Here used PVC-U pipe has Young's modulus is 2.52 GPa, Yield stress of PVC-U pipe is 107 MPa, Ultimate strength of the PVC-U pipe is also 107 MPa and poisson's ratio of the PVC-U pipe is 0.36. The CFDSCT column investigated consists of an octagonal steel tube as its outer skin layer, a circular PVC-U pipe as its inner skin layer, and high strength concrete filled in between the two layers. A total of nine CFDSCT column specimens were tested in the program. The nine specimens chosen represent different range of values in radius-to- thickness ratio, hollow section ratio, and slenderness ratio.

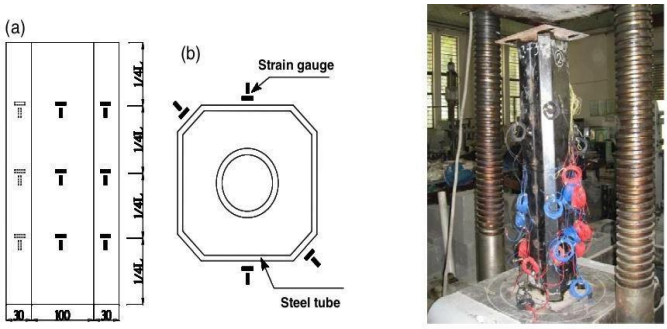

Fig 1.5- Testing equipment used in the test

The outer octagonal steel tube was made by bending a steel plate into an open-octagonal shape and then welding to form a close tube. The material properties of the steel plate used are: Young's modulus Es=210 GPa, yield strength fsy=235 MPa, ultimate strength fsu= 375 MPa, and Poisson's ratio vs=0.3.Eight steel heads welded to the inner surface of the outer skin steel tube on two sections were used to hold in position the inner PVC-U tube. The steel heads are made from the normal steel bar of diameter 6 mm. The octagonal section has combined advantages of conventional circular and square sections and thus has become popular in concrete-filled double skin tubular columns. Strain gauges were used to measure the deformations of the steel tube and PVC-U pipe. Twenty four strain gauges were located on the outside surface of the steel tube at ¼, ½ and ¾ sections At each section there were eight strain gauges, four in axial direction and four in transverse direction. These four axial (or transverse) strain gauges were placed at the two opposite long and short sides of the octagon. Two axial and two circumferential strain gauges were placed at the inner surface of the PVC-U pipe at its ½ section on each side. The TDS-300 data logger was used to collect the data from these strain gauges. Prior to testing, the top surfaces of the CFDSCT specimens were ground smooth and flat using a grinding wheel with diamond cutters. A ruler was used to check for the flatness. This was to ensure that the load was applied evenly across the cross- section and simultaneously to the steel and concrete. All tests were performed on a 2000 kN capacity universal testing machine and the test data were collected by an IMP data acquisition system. For each test the CFDSCT column specimen was placed into the testing machine and the centrally axial load was applied on the specimen directly. The loading ram was a solid steel plate. A load increment of less than one tenth of the estimated load capacity was used. The load increment was gradually achieved by controlling the axial displacement. Each load interval was maintained for about 2 to 3 min. Two displacement transducers were used to measure the axial shortening at the same time. The test was stopped when the load was found to reduce while the axial displacement continued increasing.

Objectives :- The objectives of the study is-

1) To develop a model using ABAQUS and experimental data of Concrete-Filled double skin composite tubular columns and compare the results.

International Journal of Engineering Research & Technology (IJERT)
ISSN: 2278-0181
Vol. 9 Issue 06, June-2020

2) Using the ABAQUS model, to study the effect of following variables on the behaviour of CFDSCT-
   i) Radius-to-thickness ratio
   ii) Hallow section ratio
   iii) Thickness of the PVC-U pipe

II. LITERATURE REVIEW

Dai and Lam (2010) investigated the axial compressive behaviour of short concrete-filled elliptical steel column by using ABAQUS. A new stress strain curve for hallow section confined concrete was made. The stress strain curve obtained by simulation and by experiment was compared and verified. The cross-section of elliptical hollow section was 150*75 with three different thickness 4mm, 5mm and 6.3mm and C30, C60 and C100 concrete grades were used. The load-axial shortening curve, failure modes and ultimate load capacity of the section was obtained from numerical models and compared with the experimental results.

Hou and Zhao (2005) presented the behaviour of circular concrete filled double skin tubes (CFDST) subjected to local bearing forces. The study was an extension of a previous work on concrete filled steel tubes (CFST). A finite element analysis (FEA) modelling was established and verified by the test data. Comparative analysis was conducted between the full-range behaviour of CFDST and CFST under local bearing. It was found that the performance of CFDST was considerably affected by the interaction of the outer tube, inner tube and the sandwiched concrete, whilst its bearing capacity depends on the hollow ratio.

Han and Tao (2007) studied the torsional behaviours of concrete-filled thin-walled steel tubes. ABAQUS software was used for the finite element analysis (FEA) of CFST subjected to pure torsion. A comparison of results calculated using this modelling shows good agreement with test results. The FEA modelling was used to investigate the influence of important parameters that determine the ultimate torsional strength of the composite sections. The parametric studies provided information for the development of formulae to calculate the ultimate torsional strength, as well as the torsional moment versus torsional strain curves of the composite sections.

Han and Xu (2010) tested eight FRP–concrete–steel double-skin tubular columns under constant axial load and cyclically increasing flexural loading. The main parameters in the tests were axial load level and number of fibre reinforced polymer (FRP) layers. The influence of those parameters on the strength, ductility, stiffness, and energy dissipation was investigated. It was found that, in general, FRP–concrete–steel double-skin tubular columns exhibit high levels of energy dissipation prior to the rupture of the longitudinal FRP.

Hibbitt (2010) investigated the behaviour of CFDST members under low velocity lateral impact using ABAQUS, where nonlinear material behaviour and strain rates of steel and concrete were included. The finite element analysis (FEA) models of CFDST members were described and verified using existing experimental results. Strain and stress states of concrete and steel tube in CFDST members were analyzed over the full loading range, followed by a parametric study investigating the influence of impact height, hollow ratio, nominal steel ratio, diameter-to-thickness ratio of inner steel tube and strength of materials on the impact force and global residual lateral deformation.

Han and Liao (2011) carried out a series of tests on concrete-filled double skin steel tubes (CFDST) columns under long-term sustained loading condition. The test process included two stages, i.e. long-term service test and ultimate strength test. Numerical models on analysis of the CFDST column under long-term sustained loading were presented. A comparison of results calculated using the models showed generally good agreement with the test results. Additionally, a detailed analysis was performed to analyse the long-term behaviour of CFDST columns. Finally, simplified formula for calculating the ultimate strength of CFDST columns subjected to long-term sustained loading was proposed.

Ren and Li (2011) introduced a new type of composite member, a stainless steel–concrete– carbon steel double-skin tubular (DST) column. This composite member was expected to combine the advantages of all three types of materials, and had additional advantages of aesthetics and resistance to corrosion that outer stainless steel offers. Total 80 specimens were tested. The main parameters of the tests were the sectional type (circular, square, round- end rectangular and elliptical), the column type (straight, inclined and tapered), and the hollow ratio of the composite section. The results showed that all types of columns behaved in a ductile manner, and the mechanical behaviour was similar to those columns with double carbon steel tubes.

T.H. Han, J.M. Stallings, Y.J. Kang (2010) did the double skin concrete-filled tubular column analysis by nonlinear analysis. By using the failure mode of column the stress strain diagram was made. And for each failure modes, concrete confining pressure equations were developed. Then the comparison was done between analytical result and experimental results. And finally explained the ultimate strength of double skin concrete filled tubular column was more than the sum of the ultimate strength of its components member that was inner tube, outer tube and sandwiched concrete.

Zhao and Grzebieta (2002) studied the plastic collapse behaviour of concrete-filled double skin tube column. The buckling in the outer tube was also studied. And it was found that the experimental and analytical results were matched.

III. FINITE ELEMENT ANALYSIS MODELLING

Experimental studies provide sufficient information about the structural behaviour. But sometimes it is difficult to do a lot of experiments and also it is time consuming, so fortuitously we can do the same by using quickly developed finite element analysis which is a very powerful tool for engineering researchers.

International Journal of Engineering Research & Technology (IJERT)
ISSN: 2278-0181
Vol. 9 Issue 06, June-2020

ABAQUS is divided into different functional unit called as modules. Each module has its own specific portion of modelling task. Here nine models are prepared. Modelling of outer steel is done as a solid homogenous 3D deformable. Modelling of sandwiched concrete and inner PVC pipe is also done same that is solid homogeneous 3D deformable. At the end point of the model a plate is fixed which is 3D discrete rigid, the purpose of the rigid plate is to uniformly distribute the load acting on the column.

3.1 Parts:- Parts are the building blocks of an Abaqus/CAE model.We use the Part module to creat each part, and then use the Assembly module to assemble instances of the part.Total nine models are made each of different dimensions. Specimen 1-1 is made as outer diameter of steel tube is 160mm and thickness is 3.5mm, and inner PVC pipe tube has a diameter of 75mm and has thickness of 2.3mm, and the sandwiched concrete has inner outer diameter as a 159mm and inner diameter as 74mm and the length of the specimen is 380mm. There is a small gap between the steel diameter and concrete diameter because this is not possible for both to overlap at each other.

Specimen label	D_o(mm) X T_o(mm)	D_i(mm) X T_i(mm)	Length (mm)
1-1	160X3.5	75X2.3	380
1-2	160X3.5	75X2.3	670
1-3	160X3.5	75X2.3	860
2-1	160X3	75X2.3	380
2-2	160X3	75X2.3	670
2-3	160X3	75X2.3	860
3-1	160X3	50X2.0	380
3-2	160X3	50X2.0	670
3-3	160X3	50X2.0	860

Table 3.1: Dimensions of the models

The same gap is between concrete diameter and PVC pipe diameter. Specimen 1-2, the outer diameter of steel tube is 160mm and thickness is 3.5mm, and inner PVC pipe diameter is 75mm and thickness 2.3 and length 670mm. Specimen 1-3 has the same cross section diameter only has different length that is 860mm.

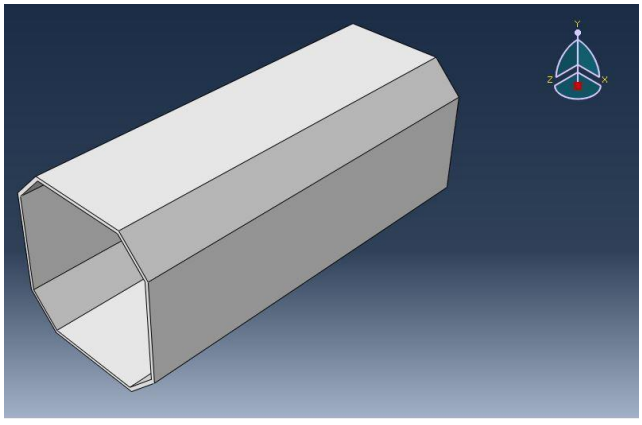

Fig 3.1: Outer steel part

Specimen 2-1, the outer diameter of steel tube is 160mm and thickness is 3mm, and inner PVC pipe diameter is 75mm and thickness 2.3 and length 380mm. Specimen 2-2 and specimen 2-3 have the same cross section dimensions only the length of the specimen are different which is 670mm and 860mm respectively. Specimen 3-1.

The outer diameter of steel tube is 160mm and thickness is 3mm, and inner PVC pipe diameter is 50mm and thickness 2 and length 380mm. Specimen 2-2 and specimen 2-3 have the same cross section dimensions only the length of the specimen are different which is 670mm and 860mm respectively

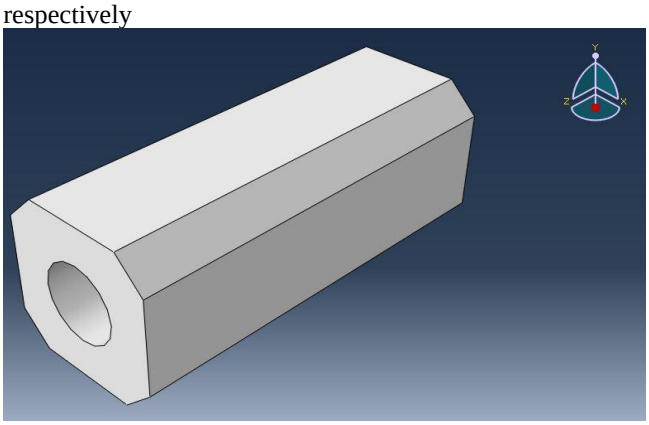

Fig3.2: Concrete part

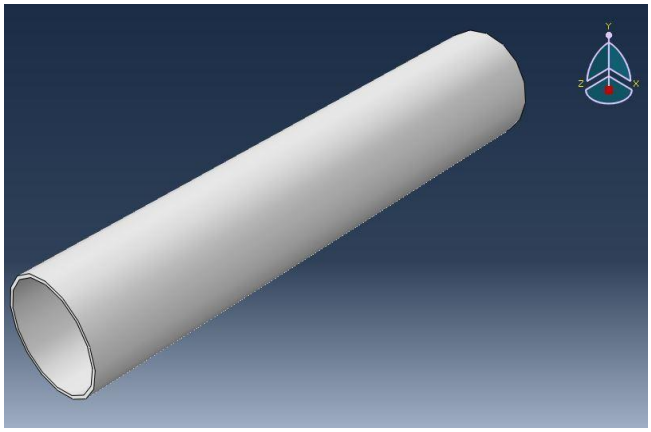

Fig 3.3: Inner PVC-U part

3.2 Properties:

Materials	Young's modulus (GPa)	Yield stress (MPa)	Ultimate strength (MPa)	Poisson's ratio
Steel	210	235	375	03
PVC-U	2.52	107	107	0.36
Concrete	36.3	Characteristics 28-day concrete cube strength f_{cu} =62.3		0.2

Table 3.2: Properties of materials

The steel which is used have the young's modulus 210 GPa, Yield stress of the steel is 235MPa, the ultimate strength of the steel is 375MPa and Poisson's ratio is 0.3 The concrete which is used have the young's modulus 36.3 GPa, the characteristics strength of concrete is 62.3MPa and Poisson's ratio is 0.2. The PVC pipe having the young's modulus of 2.52GPa , yield stress of 107MPa, ultimate strength of 107MPa and Poisson's ratio 0.36.

Concrete damage plasticity model is used for concrete and for the property of steel, Johnson- cook model is used. For PVC its conductivity and specific heat value is also taken.

International Journal of Engineering Research & Technology (IJERT)
ISSN: 2278-0181
Vol. 9 Issue 06, June-2020

Properties which are used in ABAQUS are as follows:

(A). Concrete: Density of concrete is taken as 2400 kg/m3.

Dilation Angle	Eccentricity	fb0/fc0	K	Viscosity Parameter
30	1	1.16	0.666	0.1

Table 3.3: Concrete damage parameters

Yield stress (N/m^2)	Inelastic strain
62300000	0
50000000	0.01
40000000	0.022
30000000	0.035
25000000	0.04

Table 3.4: Concrete compressive behaviour

Yield stress (N/m^2)	Cracking strain
5525000	0
4000000	0.015
3000000	0.026

Table 3.5: Concrete tensile behaviour

(B). PVC-U pipe:

Density (kg/m^3)	980
Conductivity	0.18
Specific heat	0.9

Table 3.6: Properties of PVC-U pipe

Yield stress (N/m^2)	Plastic strain
50000000	0
107000000	0.012

Table 3.7: Plastic behaviour of PVC-U pipe

(C). Steel: Density of steel is taken as 7890 Kg/m^3

d1	d2	d3	d4	d5	Melting temperature	Transition Temperature	Reference Strain Rate
0.0705	1.732	-0.54	-0.01	0	1800	293	0.0005

Table 3.8: Johnson-Cook damage parameter

A	B	n	m	Melting Temperature	Transition Temperture
490000000	383000000	0.32	0.323	1800	293

Table 3.9: Plastic behaviour of Steel (Rate dependent)

3.3 Assembly :-
In assembly module we have to assemble all the parts which are created in parts module. The outer part is octagonal steel part and the inner part is PVC-U part and the sandwiched part is concrete part. Assemble all the three parts as given in the experiment. Also assemble the upper plate at the upper portion where load is to be applied. In all three parts we have to take a small gap because in actual case there must be some gap among all the parts. The properties of each parts are assigned to each parts in property modulus. The steel part is assigned as a solid and homogenous and the material properties of steel. The concrete part is assigned as a solid and homogenous and the material properties of concrete. And the PVC-U part is also assigned as a solid and homogenous and the material properties of PVC-U.

3.4 Step: In step module for this model dynamic explicit is used. The explicit dynamics procedure performs a large number of small time increments efficiently. An explicit central-difference time integration rule is used; each increment is relatively inexpensive (compared to the direct-integration dynamic analysis procedure available in Abaqus/Standard) because there is no solution for a set of simultaneous equations. The time increment used in an analysis must be smaller than the stability limit of the central- difference operator. Failure to use a small enough time increment will result in an unstable solution. When the solution becomes unstable, the time history response of solution variables such as displacements will usually oscillate with increasing amplitudes. The total energy balance will also change significantly. If the model contains only one material type, the initial time increment is directly proportional to the size of the smallest element in the mesh. If the mesh contains uniform size elements but contains multiple material descriptions, the element with the highest wave speed will determine the initial time increment.

3.5 Interaction :- The model is made as a dynamic explicit model. The interaction between inner steel and outer concrete part is surface-to-surface interaction with frictional penalty in which the inner steel part is acts as a master surface and the outer part of concrete acts as a slave surface. The interaction between inner concrete and outer PVC is also surface.
To surface with frictional penalty in which inner part of concrete is acts as master surface and outer part of PVC acts as a slave surface.

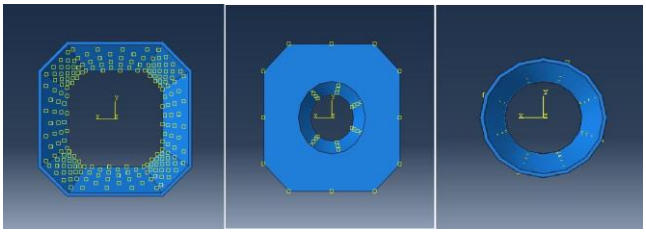

Fig3.4: Interactions between the parts

3.6 Load:- Load acting on the column is of capacity 2000kN and the 10 percent of load increases at every 2 minutes interval that is 200KN load acts for 2 minutes then increment of 200KN acts for another 2 min and increment of load is gradually. Load acts on the column on the top surface and in the form of pressure. The load acts on the top plate which distributes the load uniformly on the column The boundary condition is fixed for the bottom of the column. Rotation and displacement both are not allowed. The displacement and the rotation both are constrained in the axis at the bottom point. Fixed condition is taken because during the loading on the column, it should not rotate and displace.

International Journal of Engineering Research & Technology (IJERT)
ISSN: 2278-0181
Vol. 9 Issue 06, June-2020

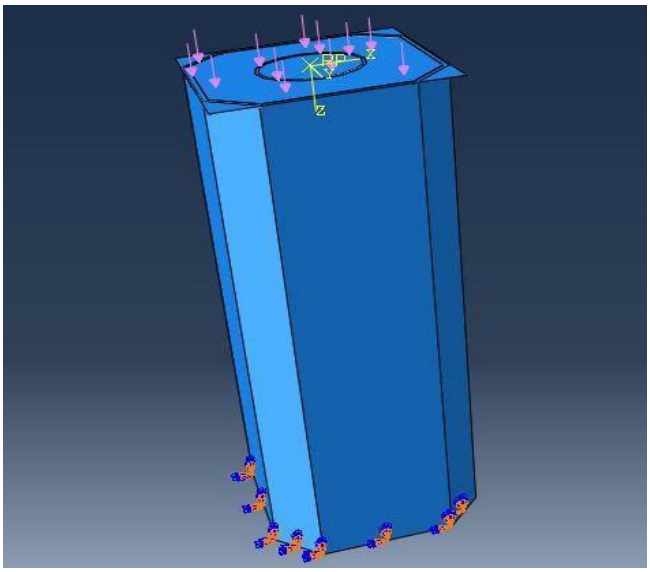

Fig 3.5: loading and boundary condition of the column

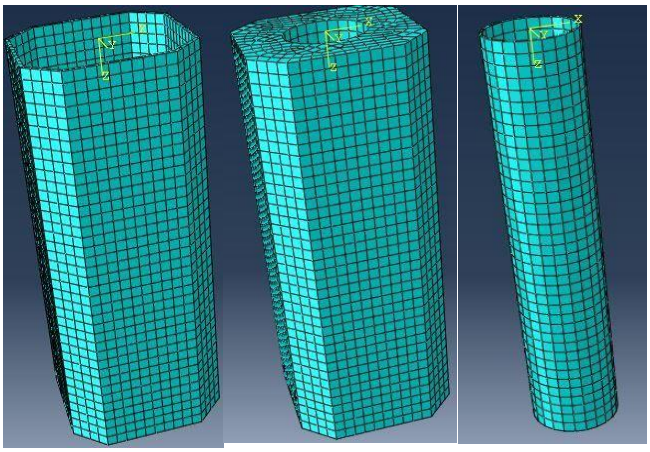

Fig 3.6: Finite element mesh for CFDSCT columns.

3.7 Mesh:- Meshing is done in the model to get accuracy in the end results. When the solid mesh approach is a course mesh, the effects are even bigger. When refine the solid mesh, the results will become more accurate. Meshes should be good enough for the analysis Meshes that are good enough are ones that produce results with an acceptable level of accuracy, assuming that all other inputs to the model are accurate. Mesh density is a significant metric used to control accuracy Assuming no singularities are present, a high-density mesh will produce results with high accuracy. However, if a mesh is too dense, it will require a large amount of computer memory and long run times.

IV. RESULT AND DISCUSSIONS

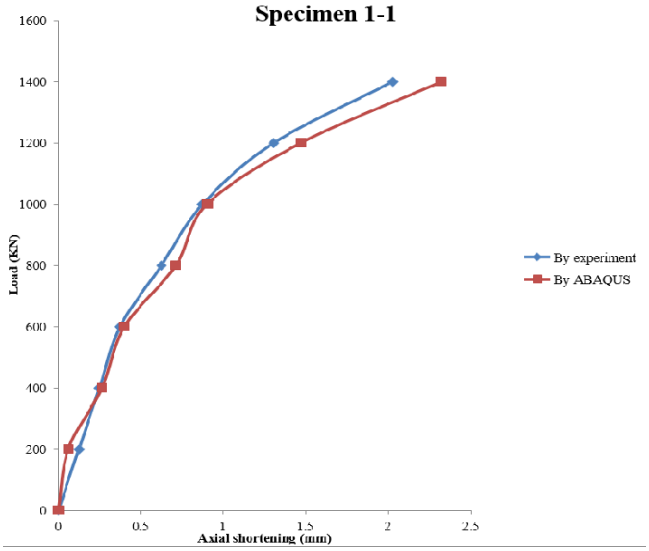

Fig 4.1:- Graph between load (KN) and axial shortening (mm) in ABAQUS and in experiment of SPECIMEN 1-1

In the above graph it is shown that for the loading of 200 KN the expeimental result shows the axial shortening of 0.125 mm and for the same load axial shoretning coming from the ABAQUS result is 0.0607 mm.

Load (KN)	Axial shortening (mm) by Experiment	Axial shortening (mm) by ABAQUS
200	0.125	0.0607
400	0.25	0.265
600	0.375	0.401
800	0.625	0.713
1000	0.875	0.902
1200	1.305	1.47
1400	2.025	2.32

Table:4.1 Axial shortening (mm) in Experiment and in ABAQUS

Relative error in experimental value and finite element analysis value Average relative error = -0.098

International Journal of Engineering Research & Technology (IJERT)
ISSN: 2278-0181
Vol. 9 Issue 06, June-2020

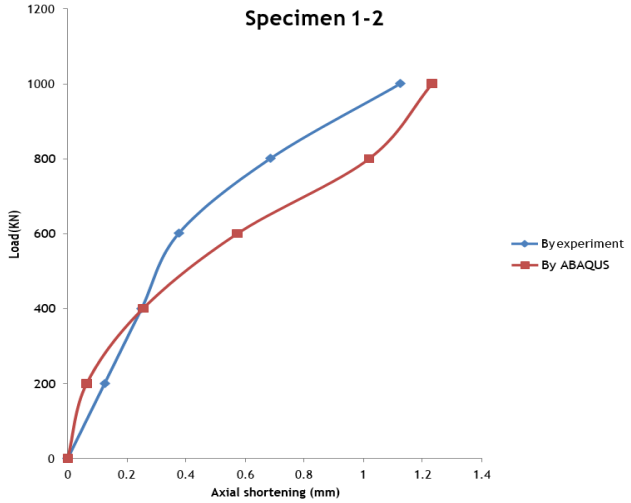

In the above graph it is shown that for the loading of 200 KN the expeimental result shows the axial shortening of 0.125 mm and for the same load axial shoretning coming from the ABAQUS result is 0.0644 mm.

Load (KN)	Axial shortening (mm) by Experiment	Axial shortening (mm) by ABAQUS
200	0.125	0.0644
400	0.25	0.255
600	0.375	0.574
800	0.685	1.02
1000	1.125	1.233

Relative error = -0.18

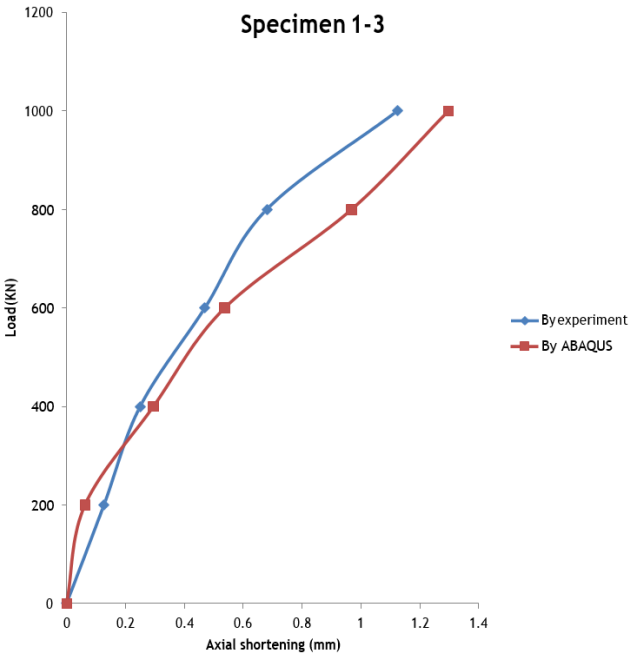

In the above graph it is shown that for the loading of 200 KN the expeimental result shows the axial shortening of 0.127 mm and for the same load axial shoretning coming from the ABAQUS result is 0.0624 mm.

Load (KN)	Axial shortening (mm) by Experiment	Axial shortening (mm) by ABAQUS
200	.127	0.0624
400	0.25	0.295
600	0.47	0.537
800	0.68	0.968
1000	1.124	1.297

Relative Error = -0.19

Fig. 4.2 Graph between load (KN) and axial shortening (mm) in ABAQUS and in experiment of SPECIMEN 2-1

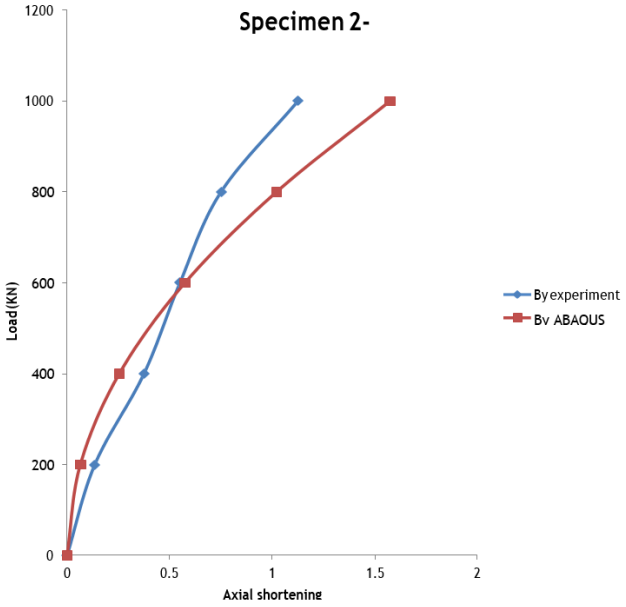

Load (KN)	Axial shortening (mm) by Experiment	Axial shortening (mm) by ABAQUS
200	0.135	0.0646
400	0.375	0.2544
600	0.55	0.5739
800	0.75	1.020
1000	1.125	1.573

Relative Error = -0.18

Fig 4.3 Graph between load (KN) and axial shortening (mm) in ABAQUS and inexperiment of SPECIMEN 2-2

In the below graph it is shown that for the loading of 200 KN the expeimental result shows the axial shortening of 0.135 mm and for the same load axial shoretning coming from the ABAQUS result is 0.0644 mm.

International Journal of Engineering Research & Technology (IJERT)
ISSN: 2278-0181
Vol. 9 Issue 06, June-2020

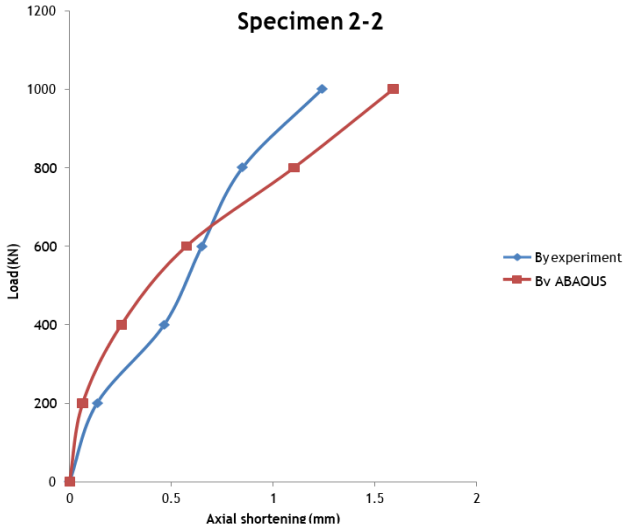

Load (KN)	Axial shortening (mm) by Experiment	Axial shortening (mm) by ABAQUS
200	0.135	0.0644
400	0.465	0.2548
600	0.65	0.5741
800	0.85	1.103
1000	1.24	1.591

Relative Error = -0.07

Fig 4.4 Graph between load (KN) and axial shortening (mm) in ABAQUS and in experiment of SPECIMEN 2-3

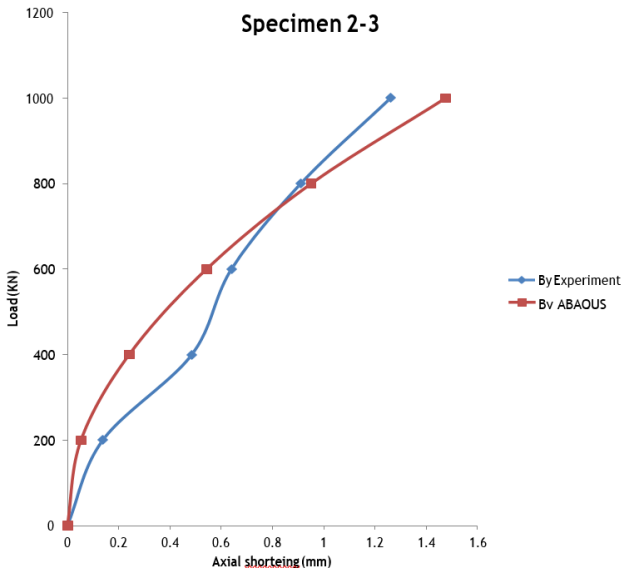

In the above graph it is shown that for the loading of 200 KN the expeimental result shows the axial shortening of 0.138 mm and for the same load axial shoretning coming from the ABAQUS result is 0.05306 mm.

Relative Error = 0.05

Load (KN)	Axial shortening (mm) by Experiment	Axial shortening (mm) by ABAQUS
200	0.138	0.05306
400	0.485	0.2406
600	0.64	0.5423
800	0.91	0.9503
1000	1.26	1.474

Fig 4.5 Graph between load (KN) and axial shortening (mm) in ABAQUS and in experiment of SPECIMEN 3-1

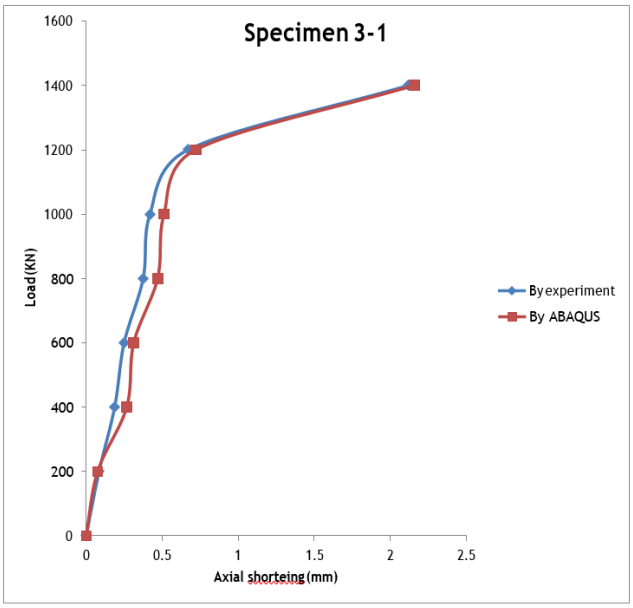

In the above graph it is shown that for the loading of 200 KN the expeimental result shows the axial shortening of 0.085 mm and for the same load axial shoretning coming from the ABAQUS result is 0.0755 mm.

International Journal of Engineering Research & Technology (IJERT)
ISSN: 2278-0181
Vol. 9 Issue 06, June-2020

Load (KN)	Axial shortening (mm) by Experiment	Axial shortening (mm) by ABAQUS
200	0.085	0.0755
400	0.1875	0.267
600	0.25	0.313
800	0.375	0.47
1000	0.42	0.512
1200	0.67	0.72
1400	2.12	2.156

Relative Error = -0.098

Fig 4.6 Graph between load (KN) and axial shortening (mm) in ABAQUS and in experiment of SPECIMEN 3-2

In the graph it is shown that for the loading of 200 KN the expeimental result shows the axial shortening of 0.085 mm and for the same load axial shoretning coming from the ABAQUS result is 0.0521 mm.

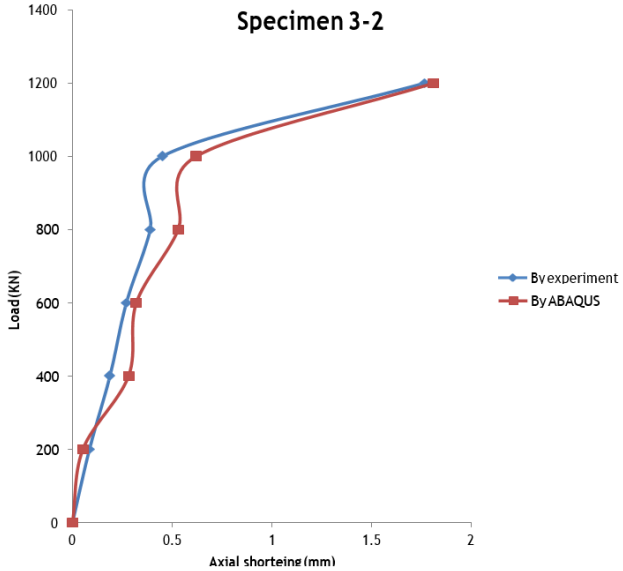

Load (KN)	Axial shortening (mm) by Experiment	Axial shortening (mm) by ABAQUS
200	0.085	0.0521
400	0.1875	0.281
600	0.27	0.32
800	0.39	0.53
1000	0.45	0.62
1200	1.765	1.81

Relative Error = -0.147

Fig 4.7 Graph between load (KN) and axial shortening (mm) in ABAQUS and in experiment of SPECIMEN 3-3

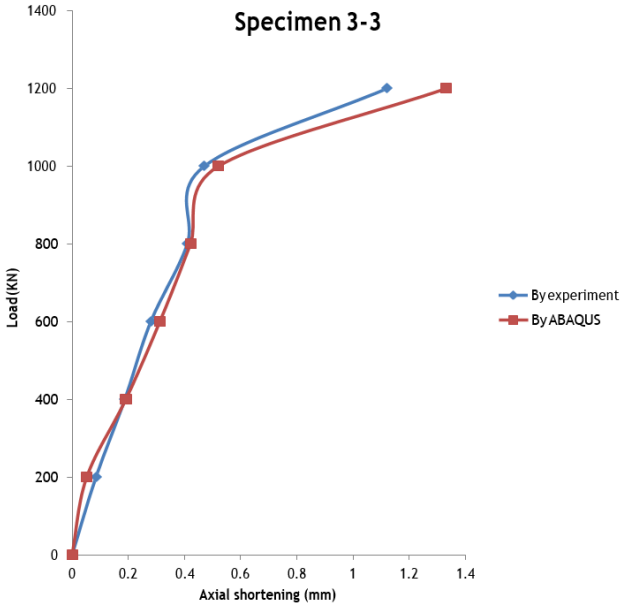

In the above graph it is shown that for the loading of 200 KN the expeimental result shows the axial shortening of 0.085 mm and for the same load axial shoretning coming from the ABAQUS result is 0.0520 mm.

Load (KN)	Axial shortening (mm) by Experiment	Axial shortening (mm) by ABAQUS
200	0.085	0.0520
400	0.1875	0.191
600	0.28	0.312
800	0.41	0.421
1000	0.47	0.52
1200	1.12	1.33

Relative Error = -0.107

4.2 Failure pattern of the CFDSCT

The final failure mode of the column is even more complicated, which is dependent on the compressive strength of steel tube, sandwiched concrete, PVC-U pipe, the slenderness of the column, the confinement effect, and the yielding of individual materials.

The failure modes observed in most of specimens were either the steel tube failure or the sandwiched concrete failure. The former was due to the combined action of axial compression and internal expansion of concrete, which may lead to the welding failure, local or global elastoplastic buckling failure of the steel tube. The latter was due to the crushing failure of concrete material, which, in turn, may lead to the failure of the outer steel tube.

International Journal of Engineering Research & Technology (IJERT)
ISSN: 2278-0181
Vol. 9 Issue 06, June-2020

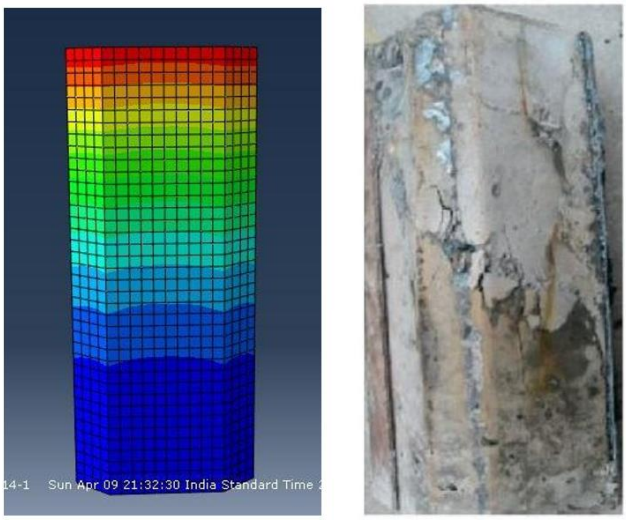

Fig 4.8 Failure Pattern of the CFDSCT by Experiment and by ABAQUS

Using the compared results of all nine models we found that there is only slight difference coming in experiment and ABAQUS load Vs axial shortening graph, and the failure pattern of CFDSCT by experiment and by ABAQUS, we can conclude that our model is correctly matched with the experimental specimens. Then now we are comparing the model for different radius to thickness ratio, different hallow section ratio and for different slenderness ratio. Using the ABAQUS model, we find the effect of following variables on the behaviour of CFDSCT-

i) radius-to-thickness ratio (α),
ii) hollow section ratio (χ),
iii) the thickness of the PVC-U pipe.

4.3 Effect of Radius to thickness ratio

It can be seen from the figure that the Ultimate load of the column decreases with the increase in radius-to-thickness ratio. Radius-to-thickness ratio is the ratio of outer diameter of the CFDSCT to the Outer thickness of the steel of CFDSCT.

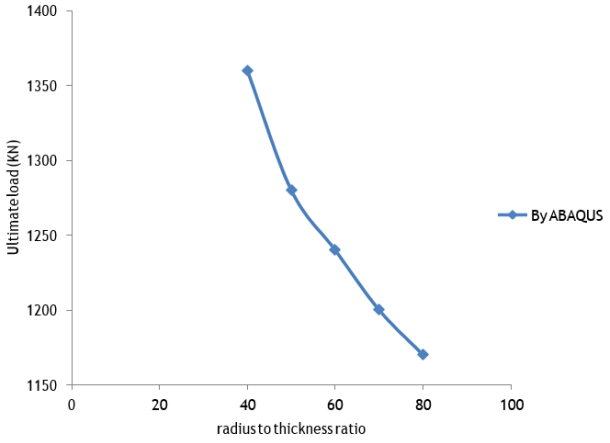

Fig 4.9 Influence of the radius-to-thickness ratio on the ultimate strength of the CFDSCT column (χ=0.49, λ=8)

4.4 Effect of hollow section ratio

It can be seen from the Graph 11 that the Ultimate load of the column decreases with the increase in hollow section ratio. Hollow section ratio is the ratio of inner diameter of PVC-U pipe to inner diameter of steel pipe in CFDSCT.

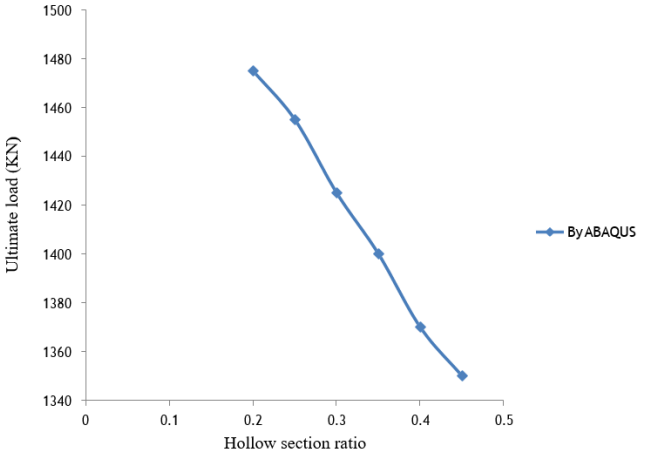

Fig 4.10 Influence of the hollow section ratio on the ultimate strength of the CFDSCT column (α=46, λ=8)

4.5 Effect of thickness of PVC-U pipe

The relationship between the ultimate compressive strength of the column and the PVC-U pipe thickness is also almost linear.

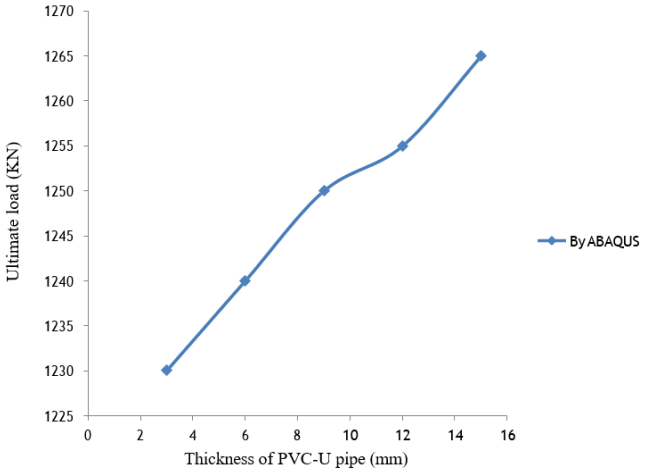

Fig 4.10 Influence of PVC-U pipe thicknesses on the ultimate strength of the CFDSCT column (Do=160 mm, Di=75 mm, to=3.5 mm, L=380 mm).

The innovation of the present study is the use of inner PVC-U pipe, instead of commonly used steel tube. The PVC-U pipe has lower strength. However, as is demonstrated above, due to relatively small cross-section area, the influence of the strength of the inner pipe on the load capacity of the whole column is not very significant. As far as the confinement is concerned, it was found from the finite element analyses that the inner pipe has almost no influence on the circumferential strain of the outer steel tube when the wall thickness of the pipe is greater than 3 mm.

International Journal of Engineering Research & Technology (IJERT)
ISSN: 2278-0181
Vol. 9 Issue 06, June-2020

CONCLUSION

(1) The values of axial shortening of different models by ABAQUS is matched with the experimental values with negligible deviation.

(2) Under the action of a compressive load, the CFDSCT column exhibits an initial linear elastic deformation, followed by a nonlinear elastoplastic deformation until the load reaches to a peak point.

(3) The increase of the wall thickness (>3 mm) of inner PVC-U pipe has almost no influence on the action to concrete confinement, although it could marginally increase the ultimate compressive load of the CFDSCT column.

(4) The ultimate load of the CFDSCT column decreases with the increase of hollow section ratio.

(5) The ultimate load of the CFDSCT column decreases with the increase of radius-to- thickness ratio.

(6) The design equation recommended matches well with both finite element results and experimental data.

This study demonstrates the possibility of using a PVC-U pipe as the inner tube in the CFDST columns. Considering the advantages of PVC-U pipes, such as cheap, good formwork, easy in construction, and the possible use as a service pipe, it is believed that the PVC-U pipe could have a good prospect for the use in practice.

REFERENCES

[1] ASTM Annual Book, Volume 08.04, Plastics Pipe and building Products, ASTM International, West Conshohocken, PA.
[2] Dai X and Lam D.(2008) Numerical modelling of axial compressive behaviour of short concrete-filled elliptical steel columns. J Constr Steel Res 66(7):931-42.
[3] Elchalakani M, Zhao XL and Grzebieta R.(2002) Tests on concrete filled double-skin (CHS outer and SHS inner) composite short columns under axial compression. Thin-Walled Struct 40(5):415-41.
[4] Han LH, Ren QX and Li W.(2012) Tests on inclined, tapered and STS concrete filled steel tubular (CFST) stub columns. J Constr Steel Res 66(10):1186-95.
[5] Han (2007) Concrete filled steel tubular columns—theory and practice (second version). Beijing: Science Press.
[6] Schneider (1998) Axially loaded concrete-filled steel tubes. J Struct Eng ASCE 124(10):1125-38.
[7] Uenaka K, Kitoh H and Sonoda K.(2010) Concrete filled double skin circular stub columns under compression. Thin-Walled Structure 48(1):19-24.
[8] Wright HD, Oduyemi TOS and Evans HR (1991) The experimental behavior of double skin composite elements. J Constr Steel Res 19(2):91–110.
[9] Wei S, Mau ST and Vipulanandan(1995) Performance of new sandwich tube under axial loading: experiment. J Struct Eng 121(12):1806-14.
[10] Wei S, Mau ST, Vipulanandan C and Mantrala SK. (1995) Performance of New Sandwich Tube under axial loading: analysis. J Struct Eng 121(12):1815-21.
[11] Yuan and Yang (2013) Experimental studies on short concrete filled double skin composite tubular column under axially compressive load.
[12] Yang JJ, Xu HY and Peng GJ.(2007) A study on the behavior of concrete-filled double skin steel tubular columns of octagon section under axial compression. China Civ Eng J 40(2):33-8.
[13] Yang H, Lam D and Gardner L.(2008) Testing and analysis of concrete-filled elliptical hollow section. Eng Struct 30(12):3771-81.
[14] Zhao XL and Grzebieta R. (2002) Strength and ductility of concrete-filled double skin (SHS inner and SHS outer) tubes. Thin-Walled Struct 40(2):199-213.
[15] Zhao XL, Han B and Grzebieta RH.(2002) Plastic mechanism analysis of concrete-filled double-skin (SHS inner and SHS outer) stub columns. Thin-Walled Struct 40(10):815-33.